Supporting Information Paragraph

Hydrotreating performance of FCC diesel and Dibenzothiophene over NiMo supported zirconium modified Al-TUD-1 catalysts

Bo Wang[†], Chengkun Xiao[†], Pengfei Li, Zhenshan Zhao, Chunming Xu, Zhen Zhao, Qian Meng, Jianmei Li, Aijun Duan*, Zhentao Chen*

[1]State Key Laboratory of Heavy Oil Processing, China University of Petroleum, Beijing, 102249, P. R. China

[†] These authors contributed equally to this work

*Corresponding author: duanaijun@cup.edu.cn; czt@cup.edu.cn

Figure & Table Captions

Figure S1. Wide-angle XRD pattern of AT-x and γ-Al_2O_3 material.

Figure S2. (A) the nitrogen adsorption-desorpotion isotherms and (B) pore diameter distribution of Al-TUD-1 series materials.

Figure S3. TEM image of AT (A) and ZrAT-25 (B).

Figure S4. Wide-angle XRD patterns of NiMo/ZrAT-x and NiMo/ZrO_2 catalysts.

Figure S5. N_2 isotherm curves (A) and pore size distributions (B) of NiMo/ZrAT-x catalysts.

Figure S6. EDX characterizations of (A) NiMo/ZrAT-25 and (B) NiMo/AT catalysts.

Figure S7. Zr3d XPS spectra of (A) NiMo/ZrAT-5, (B) NiMo/ZrAT-10, (C) NiMo/ZrAT-25, (D) NiMo/ZrAT-50, (E) NiMo/ZrAT-100, (F) NiMo/ZrAT-25 sulfided catalysts.

Figure S8. The pyridine IR spectra of (a) NiMo/AT, (b) NiMo/ZrAT-100, (c) NiMo/ZrAT-50, (d) NiMo/ZrAT-25, (e) NiMo/ZrAT-10, and (f) NiMo/ZrAT-5 after degassing at (A) 473 K and (B) 623 K.

Figure S9. The phase equilibrium image of decalin under the reaction conditions.

Figure S10. HDS results of NiMo/ZrAT-5 and NiMo/Al_2O_3 catalysts at different WHSVs (613 K, 6 MPa, 200 ml/ml).

Figure S11. The product distribution in the HDS of DBT over NiMo/ZrAT-100 at different WHSVs (573 K, 6 MPa, 200 ml/ml).

Figure S12. The product distribution in the HDS of DBT over NiMo/ZrAT-100 at different temperatures (100 h^{-1}, 6 MPa, 200 ml/ml).

Figure S13. The product distributions in the HDS of DBT over different catalysts at about 50 % of the total DBT conversion..

S1. XRD of AT-x material with different thermal treatment times

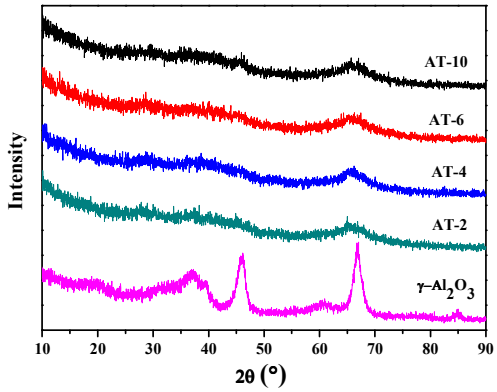

Figure S1. Wide-angle XRD pattern of AT-x and γ-Al_2O_3 material

S2. BET characterization of AT-x material with different thermal treatment times

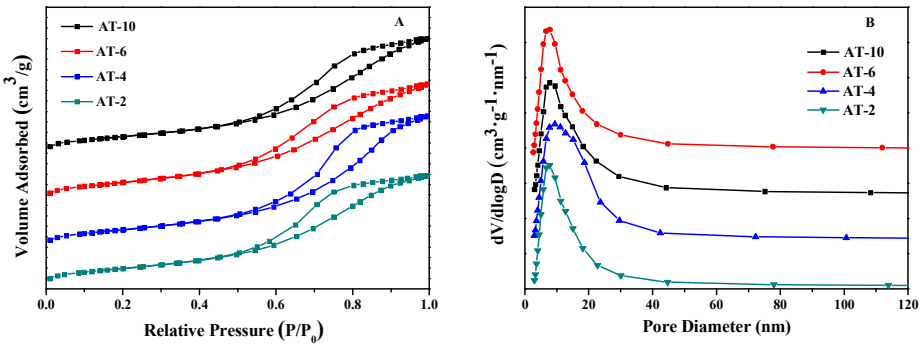

Figure S2. (A) the nitrogen adsorption-desorpotion isotherms and (B) pore diameter distribution of Al-TUD-1 series materials

Table S1. Textural properties of Al-TUD-1 series materials with different heating times

Materials	S_{BET} (m^2 g^{-1})	V_{BJH} (cm^3 g^{-1})	Pore diameter (nm)
AT-10h	381	0.82	7.4
AT-6h	403	0.82	8.2
AT-4h	409	0.86	9.6
AT-2h	396	0.76	7.2

S3. TEM characterization of ZrAT-x materials

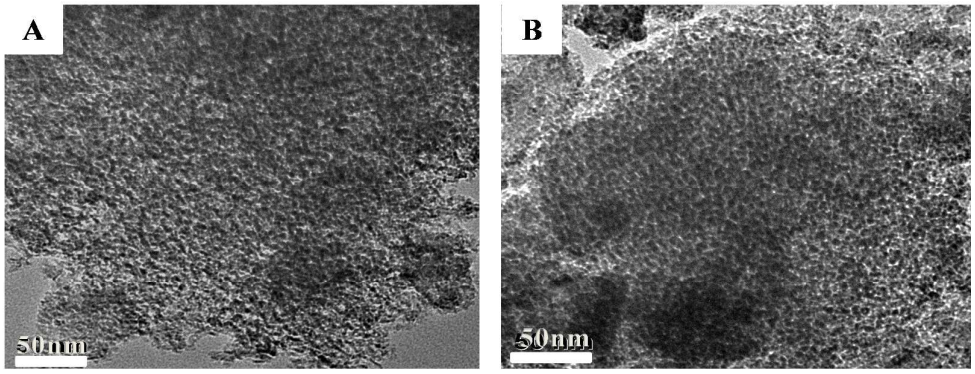

Figure S3. TEM image of AT (A) and ZrAT-25 (B)

S4. Wide-angle XRD characterization of NiMo/ZrAT-x catalysts

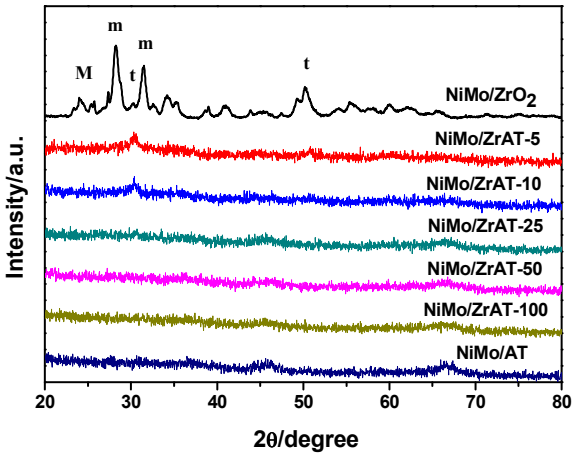

Figure S4. Wide-angle XRD patterns of NiMo/ZrAT-x and NiMo/ZrO_2 catalysts

S5. BET characterization of NiMo/ZrAT-x catalysts

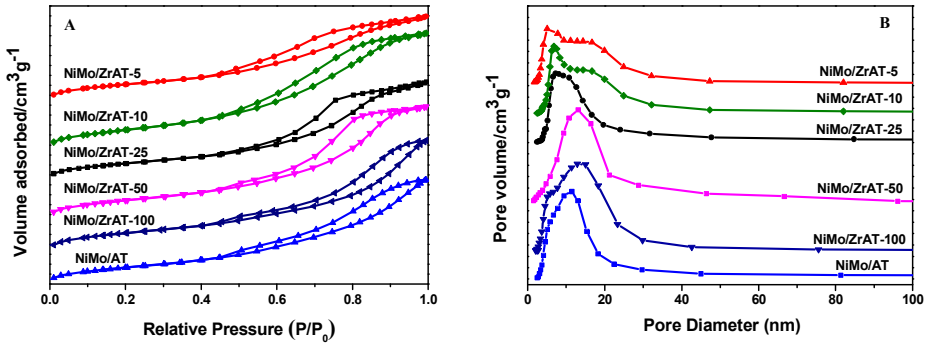

Figure S5. N_2 isotherm curves (A) and pore size distributions (B) of NiMo/ZrAT-x catalysts

Table S2. Textural properties of the NiMo/ZrAT-x catalysts

Materials	Weight percentage of ZrO_2 (%)	Al/Zr	S_{BET} (m^2 g^{-1})	V_{BJH} (cm^3 g^{-1})	Pore diameter (nm)
NiMo/ZrAT-5	32.6	5	221	0.29	8.5
NiMo/ZrAT-10	18.5	10	237	0.33	9.5
NiMo/ZrAT-25	8.8	25	252	0.38	12.8
NiMo/ZrAT-50	4.6	50	264	0.40	14.5
NiMo/ZrAT-100	2.4	100	268	0.41	15.9
NiMo/AT	0	∞	266	0.47	13.4

S6. SEM-EDS

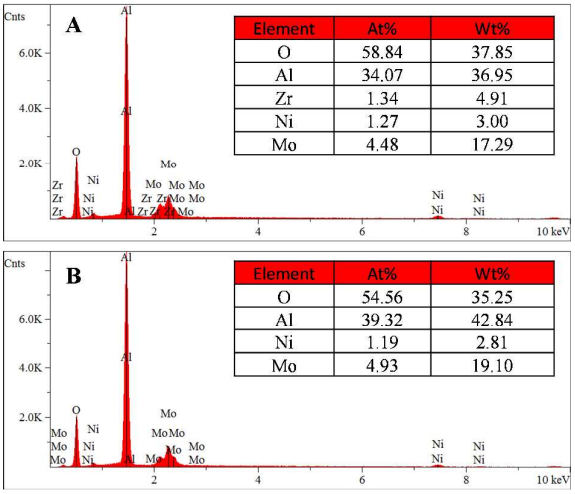

Element	At%	Wt%
O	58.84	37.85
Al	34.07	36.95
Zr	1.34	4.91
Ni	1.27	3.00
Mo	4.48	17.29

Element	At%	Wt%
O	54.56	35.25
Al	39.32	42.84
Ni	1.19	2.81
Mo	4.93	19.10

Figure S6. EDX characterizations of (A) NiMo/ZrAT-25 and (B) NiMo/AT catalysts

.

S7. XPS

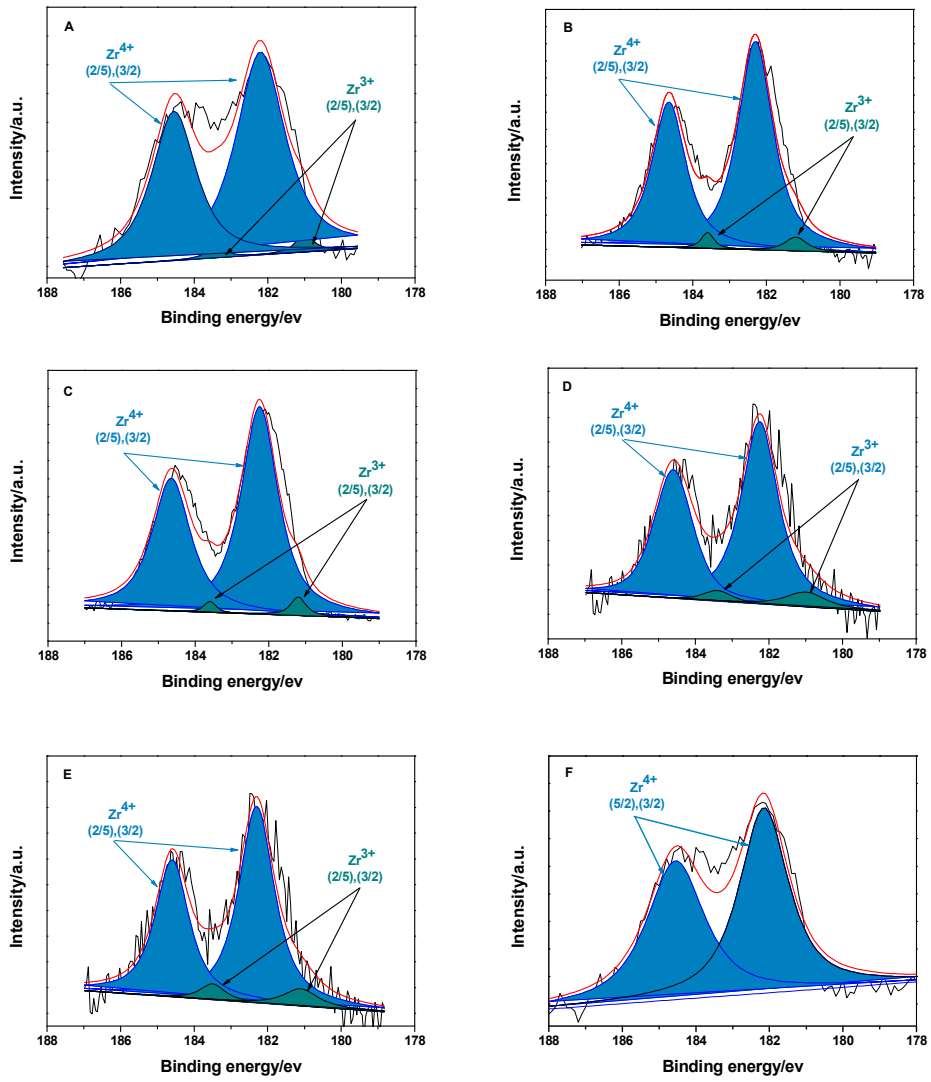

Figure S7. Zr3d XPS spectra of (A) NiMo/ZrAT-5, (B) NiMo/ZrAT-10, (C) NiMo/ZrAT-25, (D) NiMo/ZrAT-50, (E) NiMo/ZrAT-100, (F) NiMo/ZrAT-25 sulfided catalysts

Table S3. XPS fitting results of Mo 3d spectra of the sulfided catalysts

Catalysts	Mo^{4+}		Mo^{5+}		Mo^{6+}		$Mo_{sulfidity}$[a]
	ar.% (228.6 ev)	ar.% (231.7 ev)	ar.% (230.1 ev)	ar.% (233.2 ev)	ar.% (232.5 ev)	ar.% (235.6 ev)	
NiMo/ZrAT-100	34.5	23.0	6.8	4.5	18.8	12.5	57.5
NiMo/ZrAT-50	32.6	21.7	5.9	4.0	21.4	14.4	54.3
NiMo/ZrAT-25	31.9	21.3	11.1	7.4	17.1	11.4	53.2
NiMo/ZrAT-10	28.5	19.0	7.1	4.7	24.4	16.3	47.5
NiMo/ZrAT-5	26.5	17.7	2.9	1.9	30.6	20.4	44.2
NiMo/AT	15.3	10.2	18.6	12.4	26.1	17.4	25.5

[a] $S_{Mo}=Mo^{4+}/Mo_{total}$

Table S4. XPS fitting results of Ni 2p spectra of the sulfided catalysts

Catalysts	$Wt\%_{ZrO2}$	NiMoS ar.%	NiS ar.%	NiO ar.%	$Ni_{sulfidity}$[a]
NiMo/ZrAT-100	2.4	58.8	11.1	30.1	69.9
NiMo/ZrAT-50	4.6	53.7	12.1	34.2	65.8
NiMo/ZrAT-25	8.8	49.7	14.1	36.2	63.8
NiMo/ZrAT-10	19.5	39.8	14.3	45.9	54.1
NiMo/ZrAT-5	32.6	39.3	12.8	47.9	52.1
NiMo/AT	0	36.8	13.4	49.8	50.2

[a] $Ni_{sulfidity} = (NiMoS+NiS_x)/Ni_{total}$

S8. HRTEM

Table S5. Averge length and averge layer number of MoS_2 crystillates

Catalyst	L_{av} (nm)	N_{av}	f_{Mo}
NiMo/AT	3.39	2.26	0.30
NiMo/ZrAT-100	3.11	2.50	0.35
NiMo/ZrAT-50	3.18	2.65	0.34
NiMo/ZrAT-25	3.22	2.67	0.33
NiMo/ZrAT-10	3.29	2.89	0.30
NiMo/ZrAT-5	3.35	3.02	0.28

S9. Py-FTIR

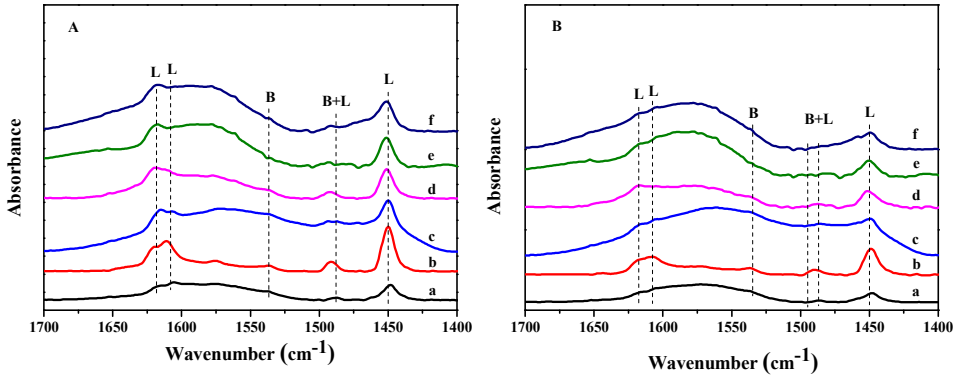

Figure S8. The pyridine IR spectra of (a) NiMo/AT, (b) NiMo/ZrAT-100, (c) NiMo/ZrAT-50, (d) NiMo/ZrAT-25, (e) NiMo/ZrAT-10, and (f) NiMo/ZrAT-5 after degassing at (A) 473 K and (B) 623 K

Table S6. The amounts of Brönsted and Lewis acid determined by pyridine-FT-IR of the different catalysts

Catalysts	473 K Acid sites (μmol g^{-1})				623 K Acid sites (μmol g^{-1})			
	B	L	L+B	B/L	B	L	L+B	B/L
NiMo/ZrAT-5	2.43	41.57	44.00	0.058	1.00	17.90	18.90	0.056
NiMo/ZrAT-10	2.80	42.86	45.66	0.065	1.10	18.31	19.41	0.060
NiMo/ZrAT-25	3.30	44.80	48.10	0.074	1.20	18.91	20.11	0.063
NiMo/ZrAT-50	3.41	47.20	50.61	0.072	1.41	22.11	23.52	0.064
NiMo/ZrAT-100	4.00	55.47	59.47	0.072	2.02	23.38	25.40	0.086
NiMo/AT	0.88	24.86	25.74	0.035	0.55	7.91	8.46	0.069

S10. Hydrotreating performance of FCC diesel

Table S7. The typical property of diesel feedstock

Properties	Data
Density @ 293K, $kg \cdot cm^{-3}$	0.87
N, $\mu g \cdot ml^{-1}$	640.3
S, $\mu g \cdot ml^{-1}$	1013
cetane number	37.7
Hydrocarbon type	
Saturated hydrocarbon (v%)	39.3
Arene (v%)	49.0
Olefin (v%)	11.7
Engler Distillation (K)	
IBP	417
5%	450
10%	464
30%	488
50%	513
70%	545
90%	583
95%	598
FBP	599

Note: IBP & FBP are the abbreviations of initial boiling point final boiling poi

Table S8. Textual properties of NiMo/γ-Al_2O_3 catalyst

Catalyst	S_{BET} (m^2 g^{-1})	V_{BJH} (cm^3 g^{-1})	Pore diameter (nm)
NiMo/γ-Al_2O_3	167	0.30	8.3
NiMo/Zr-SBA-15	447	0.72	9.6

Table S9. Acid properties of NiMo/γ-Al_2O_3 catalyst

Catalysts	473 K			623 K		
	Acid sites (μmol g^{-1})			Acid sites (μmol g^{-1})		
	B	L	L+B	B	L	L+B
NiMo/γ-Al_2O_3	0	80	80	0	26	26

Table S10. HDS activities of NiMo/ZrAT-x series catalysts

Catalysts[1]	ZrO_2, wt%	Sulfur content (mg•L^{-1})	HDS (%)	Nitrogen content (mg•L^{-1})	HDN (%)
NiMo/ZrAT-5	32.6	24.9	97.5	26.7	95.8
NiMo/ZrAT-10	19.5	22.4	97.8	20.8	96.7
NiMo/ZrAT-25	8.8	16.8	98.3	15.5	97.6
NiMo/ZrAT-50	4.6	11.9	98.8	10.7	98.3
NiMo/ZrAT-100	2.4	8.6	99.1	8.5	98.7
NiMo/AT	-	38.2	96.2	37.8	94.1
NiMo/γ-Al_2O_3	-	57.0	94.4	41.7	93.5

[1] Catalyst = 81 wt% supports + 15.5 wt% MoO_3 + 3.5 wt% NiO

S11. HDS results of DBT

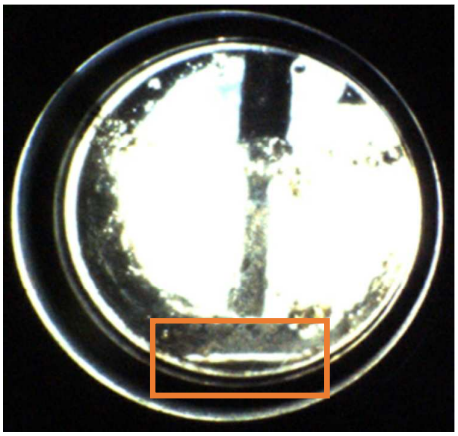

Figure S9. The phase equilibrium image of decalin under the reaction conditions

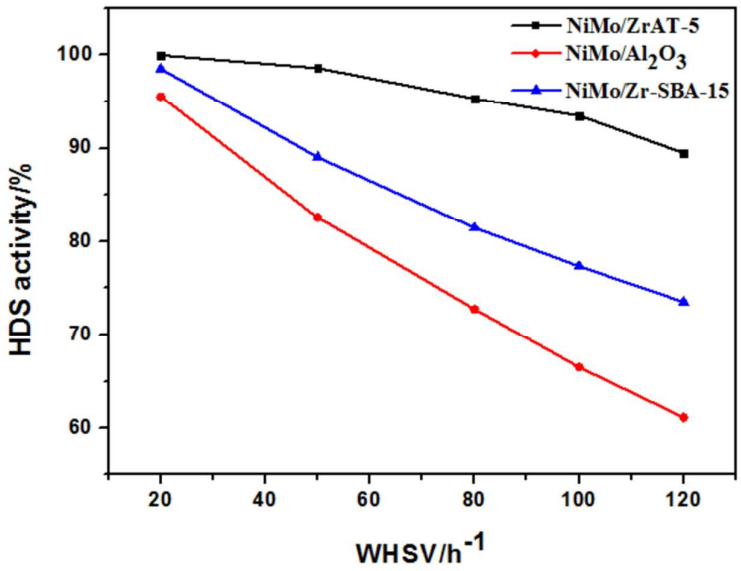

Figure S10. HDS results of NiMo/ZrAT-5 and NiMo/Al_2O_3 catalysts at different WHSVs (613 K, 6 MPa, 200 ml/ml)

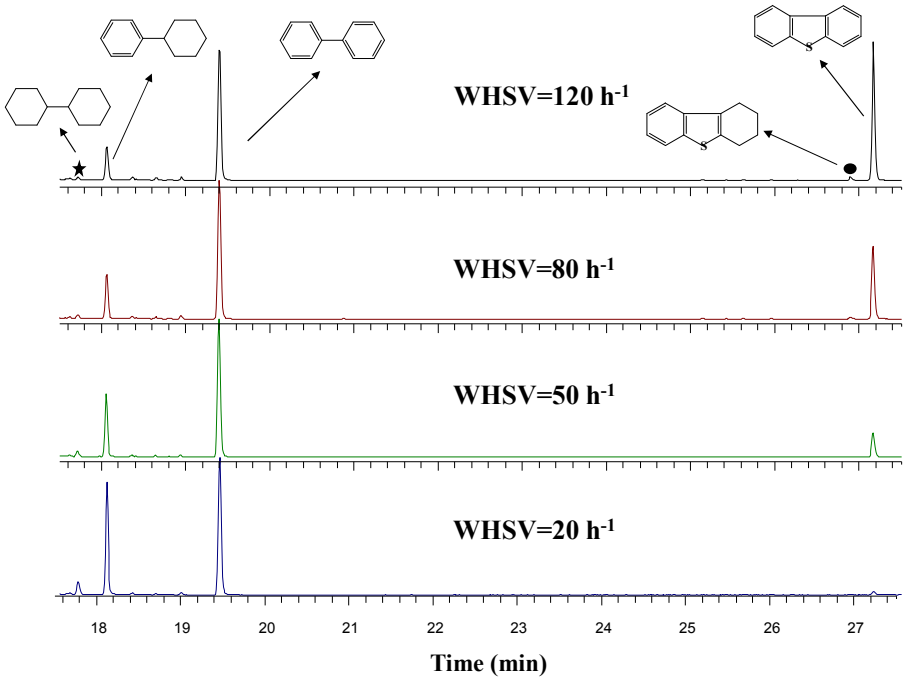

Figure S11. The product distribution in the HDS of DBT over NiMo/ZrAT-100 at different WHSVs (573 K, 6 MPa, 200 ml/ml)

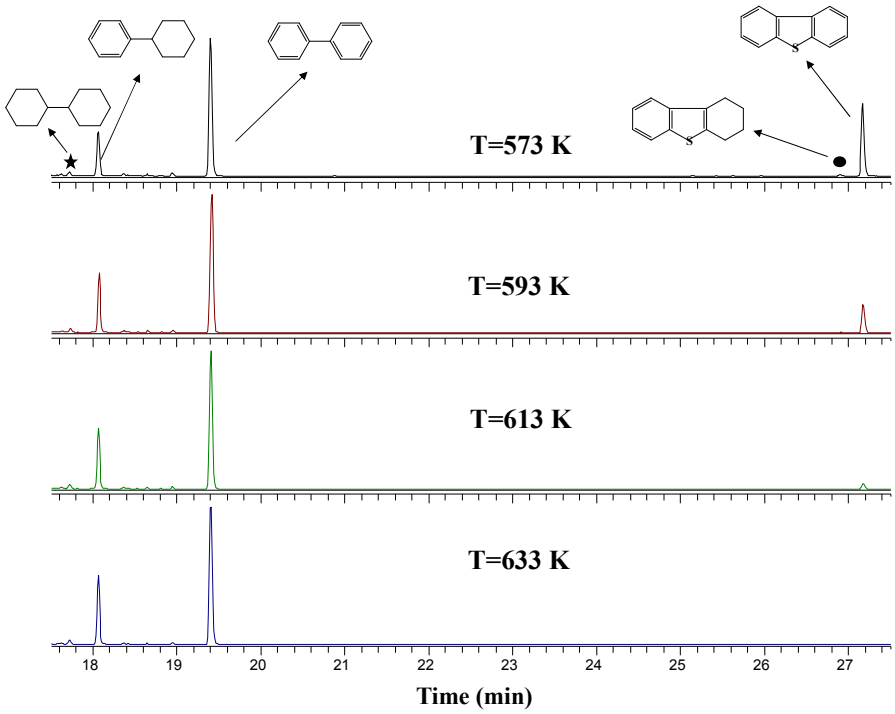

Figure S12. The product distribution in the HDS of DBT over NiMo/ZrAT-100 at different temperatures (100 h^{-1}, 6 MPa, 200 ml/ml)

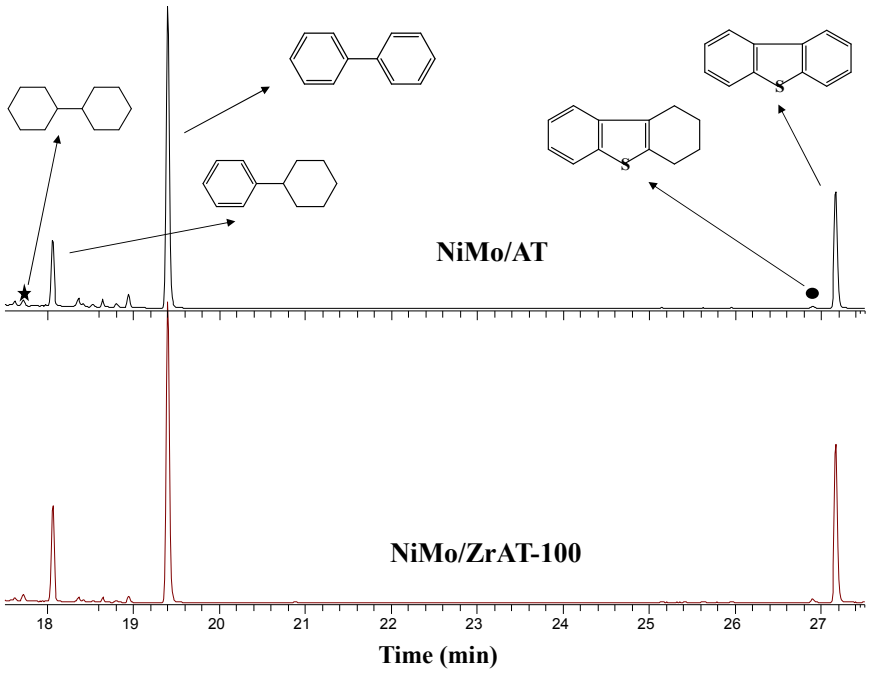

Figure S13. The product distributions in the HDS of DBT over different catalysts at about 50 % of the total DBT conversion.

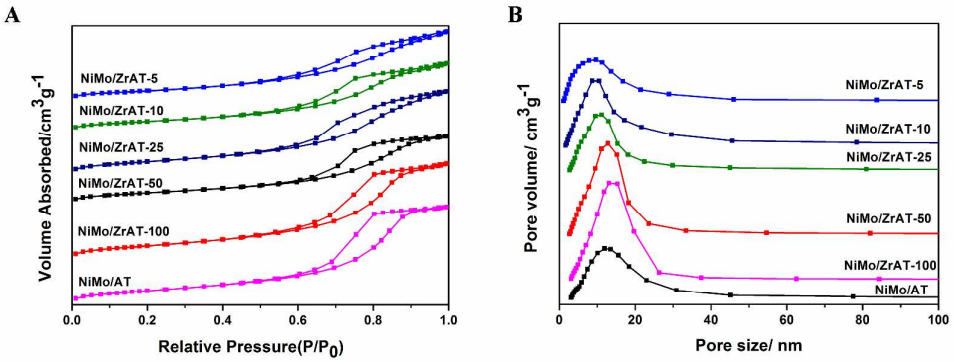

Figure S14. N_2 isotherm curves (A) and pore size distributions (B) of the used NiMo/ZrAT-x catalysts

Table S11. Textural properties of the used NiMo/ZrAT-x catalysts

Materials	Weight percentage of ZrO_2 (%)	Al/Zr	S_{BET} (m^2 g^{-1})	V_{BJH} (cm^3 g^{-1})	Pore diameter (nm)
NiMo/ZrAT-5	32.6	5	197	0.25	8.2
NiMo/ZrAT-10	18.5	10	208	0.29	9.4
NiMo/ZrAT-25	8.8	25	223	0.33	11.6
NiMo/ZrAT-50	4.6	50	239	0.37	13.8
NiMo/ZrAT-100	2.4	100	243	0.39	15.2

NiMo/AT	0	∞	238	0.43	12.5

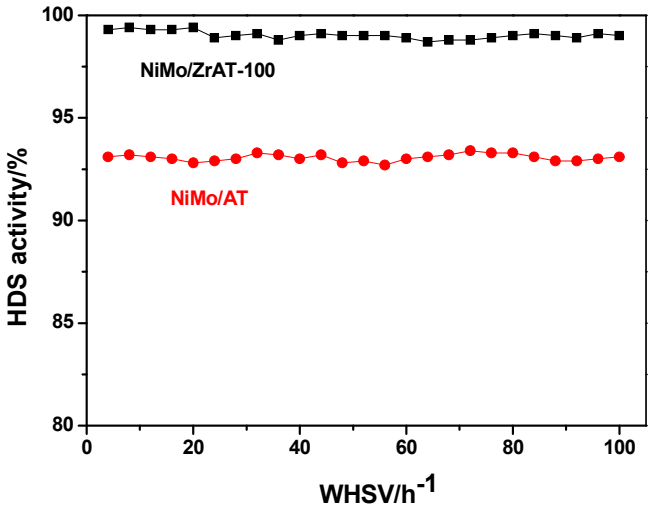

Figure S15. Time on stream over NiMo/ZrAT-100 and NiMo/AT catalysts (573 K, 6 MPa, 200 ml/ml)

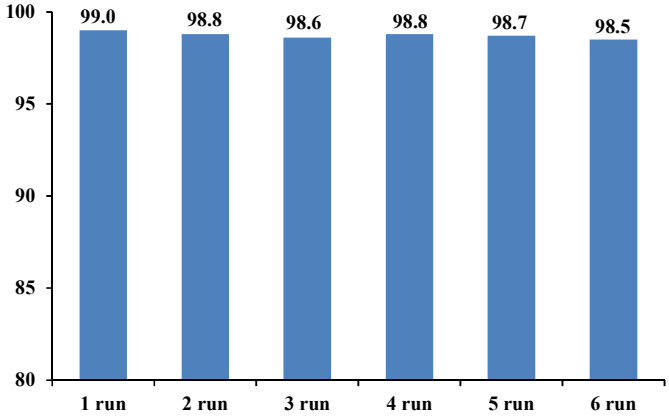

Figure S16. HDS efficiencies of NiMo/ZrAT-100 obtained at 6-run operations (20 h^{-1}, 573 K, 6 MPa, 200 ml/ml)